

## Research Article

# Structure and Physical Properties of Polymer Composite Films Doped with Fullerene Nanoparticles

R. M. Ahmed<sup>1</sup> and S. M. El-Bashir<sup>2,3</sup>

<sup>1</sup>Department of Physics, Faculty of Science, Zagazig University, Zagazig 44519, Egypt

<sup>2</sup>Department of Physics and Astronomy, Science College, King Saud University Riyadh 11451, Saudi Arabia

<sup>3</sup>Department of Physics, Faculty of Science, Banha University, Egypt

Correspondence should be addressed to R. M. Ahmed, rania8\_7@hotmail.com

Received 3 July 2010; Accepted 30 September 2010

Academic Editor: Mohamed Sabry Abdel-Mottaleb

Copyright © 2011 R. M. Ahmed and S. M. El-Bashir. This is an open access article distributed under the Creative Commons Attribution License, which permits unrestricted use, distribution, and reproduction in any medium, provided the original work is properly cited.

Fullerene C<sub>60</sub> has stimulated intense interest for scientific, industrial, and medical community because of its unique structure and properties. In the present study we prepared fullerene-doped nanocomposite films based on PMMA, PVAc, and PMMA/PVAc blend. Observations made by transmission electron microscope (TEM) showed the uniform dispersion of C<sub>60</sub> nanoparticles in the polymer matrices. Also, X-ray diffraction measurements indicated that C<sub>60</sub> has a tendency to form crystallites in the polymer matrices. In addition, the concentration effect of fullerene C<sub>60</sub> was investigated using optical absorption and photoluminescence spectroscopy. The spectroscopic properties of such films recommended their application in photonics and solar energy conversion.

## 1. Introduction

Recently, polymers are finding an important place in different research laboratories for the study of their various properties [1]. Many polymers have been proved suitable matrices in the development of composite structures due to their ease production and processing, good adhesion with reinforcing elements, resistance to corrosive environment, light weight, and in some cases ductile mechanical performance [2]. Fullerenes have been widely studied due to their unique structural, electronic and spectroscopic properties, which may be exploited for their diverse applications in chemistry, biology, and nanoscience [3].

Lately interest of researchers engaged in different fields of knowledge is seen to be focused on determination of the action of nanomaterial addition, such as fullerenes and nanotubes, on properties of polymers and their compositions. Incorporation of fullerene and nanotubes into chemical composition of polymers gives one more opportunities for their study and application as composite materials, films, and fibers serving different purposes [4].

Also, the research of polymer material has been directed to blend or copolymer of different polymers to obtain

new products having some of the desired properties of each component [5]. PMMA (polymethylmethacrylate) and its derivatives are known for their medical applications, particularly for hard tissue repair and regeneration. PMMA and (polyvinyl acetate) PVAc form an important and unique pair of polymers although they are chemically different [6].

The aim of the present work concerns on studying the change in the optical absorption, the optical parameters and photoluminescence spectra for the samples of fullerene polymer composites which are recorded at room temperature. In addition, X-ray diffraction (XRD) and transmission electron microscope (TEM) are used to characterize the fullerene/Polymer nanocomposites.

## 2. Materials and Methods

**2.1. Materials.** Both PMMA (poly methyl methacrylate) and PVAc (poly vinyl acetate) used in this study were obtained from Sigma-Aldrich (Germany) and were reported to have molecular weights of 996,000 and 167,000 g·mol<sup>-1</sup>, respectively. Moreover, Buckminster fullerene powder C<sub>60</sub>, has purity of 97% and Mr = 720.66 and was obtained from Fluka (USA). In addition, chloroform has purity of 99.8%

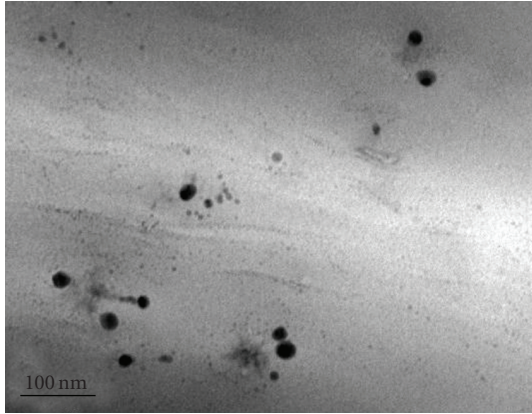


FIGURE 1: The TEM photograph of fullerene  $C_{60}$  doped in (50/50 PMMA/PVAc) blend.

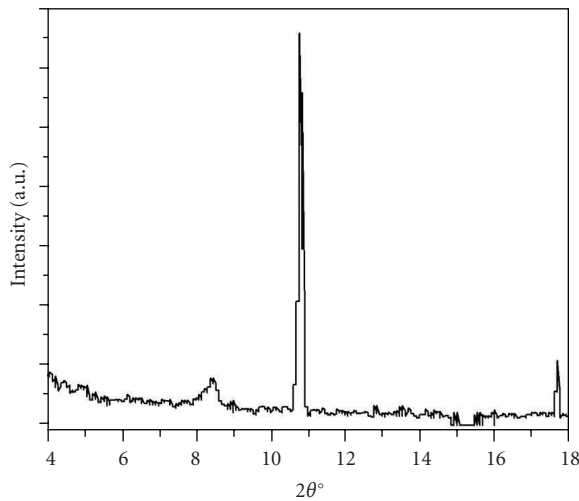


FIGURE 2: X-ray diffraction patterns of (50/50 PMMA/PVAc) blend doped with  $1 \times 10^{-4}$  of fullerene  $C_{60}$ .

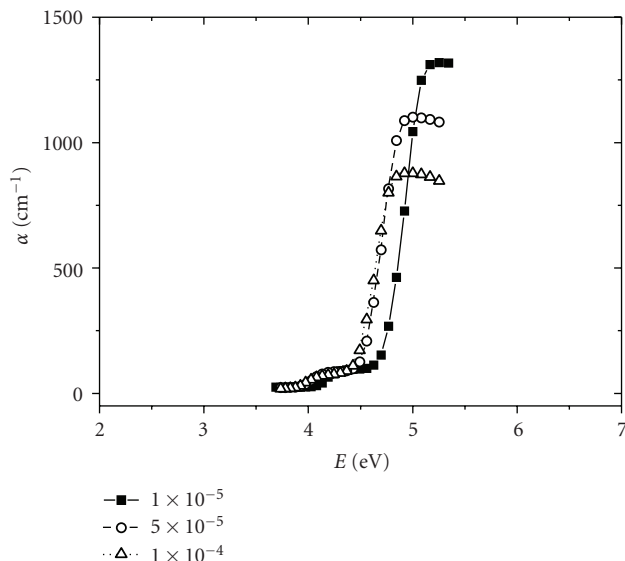


FIGURE 3: Absorption coefficient as a function of photon energy for different concentration of fullerene doped PMMA.

(HPLC) was used as a common solvent for PVAc, PMMA, and  $C_{60}$ .

**2.2. Preparation of the Samples.** Composite films (thickness  $60 \pm 10 \mu\text{m}$ ) of PMMA, PVAc and a blend of (PMMA/PVAc 50/50) doped with  $C_{60}$  were prepared by using solution-cast technique. PMMA, PVAc, and  $C_{60}$  were dissolved separately in chloroform and stirred for 48 h at  $40^\circ\text{C}$ . After that,  $C_{60}$  was mixed with homopolymers and also in their blend with different concentrations and subsequently cast onto glass dishes and then left to be dry. After drying, the films were removed and heated at  $100^\circ\text{C}$  to evaporate the confined solvent molecules. The concentrations of  $C_{60}$  in the two homopolymers and their blend are  $1 \times 10^{-5}$ ,  $5 \times 10^{-5}$  and  $1 \times 10^{-4}$  mol. %.

**2.3. Film Characterization.** TEM was performed by Transmission Electron Microscope, JEOL JEM-1400, Japan. X-ray diffraction patterns were recorded by using a Philip XRD-500 X-ray diffraction analyzer with nickel-filtered Cu-K $\alpha$  radiation at 30 kV and 20 mA.

**2.4. Spectroscopic Properties.** The absorption spectra were recorded using a UV-VIS spectrophotometer (UNICAM, Helios Co., Germany) in a range of wavelength from 190 to 900 nm. Spectrofluorimeter (Shimadzu RF-5301, PC, Japan) has been used for recording the photoluminescence spectra of  $C_{60}$  doped in PMMA, PVAc, and a blend of them. The samples were measured at room temperature and at an excitation wavelength of 400 nm.

### 3. Results and Discussion

**3.1. Characterization of the Samples.** Figure 1 presents the TEM photograph of fullerene  $C_{60}$  molecules dispersed in (50/50 PMMA/PVAc) blend, it is clear that  $C_{60}$  nanocrystals have a spherical shape. Figure 2 shows the XRD pattern for fullerene nanocrystals, sharp peaks are clearly noticed characterizing fullerene  $C_{60}$  at  $2\theta \sim 10.8^\circ$  and also at  $\sim 17.7^\circ$  in agreement with the literature [7, 8]. XRD results show that  $C_{60}$  embedded in the polymer blend are very prone to coalesce into crystallites [7].

**3.2. Fundamental Absorption Edge.** The variation of the optical bulk absorption coefficient,  $\alpha$ , with wavelength is a unique parameter of the medium, it provides the most valuable optical information available for material identification. The absorption coefficient ( $\alpha$ ) at angular frequency ( $\omega$ ) of radiation was calculated using [9]

$$\alpha(\nu) = \frac{[2.303P]}{d}, \quad (1)$$

where  $P$  is the absorbance and  $d$  is the film thickness. The fundamental absorption edge is one of the most important features of the absorption spectrum of crystalline and amorphous materials. The increased absorption near the edge is due to the generation of neutral excitations

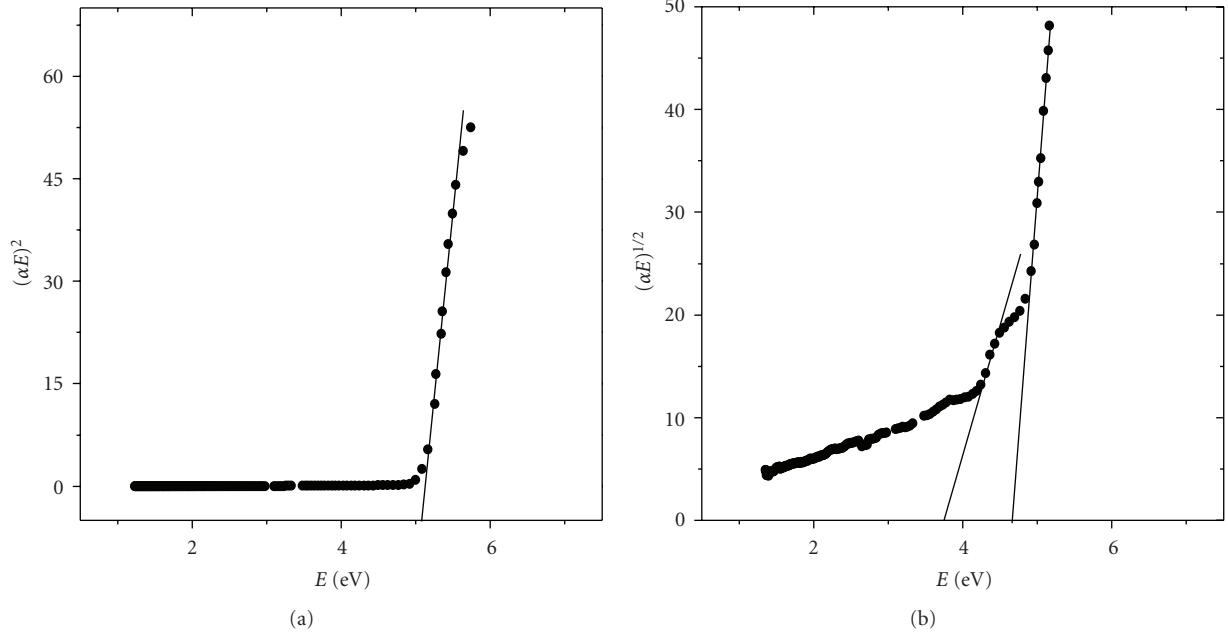


FIGURE 4: Dependence of  $(\alpha h\nu)^2$  and  $(\alpha h\nu)^{1/2}$  on photon energy ( $E = h\nu$ ) for a concentration of fullerene  $1 \times 10^{-5}$  doped in (50/50 PMMA/PVAc) blend.

and/or the transition of electrons from the valence band to the conduction band [10, 11]. Plotting the absorption coefficient against photon energy for different concentration of fullerene doped the polymer illustrates that the absorption coefficient exhibits a steep rise near the absorption edge and also a straight line relationship is observed in the high  $\alpha$ -region as seen in Figure 3. It is clear that the value of the absorption edge decreases with increasing the fullerene concentration doped in the polymer. The intercept of extrapolation to zero absorption with photon energy axis is taken as the value of absorption edge [12].

**3.3. Optical Band Gaps.** The fundamental absorption is related to band-to-band transitions, and is subject to certain selection rules [13]. The usual method to determine the energy of the band gap is to plot a graph between  $(\alpha h\nu)^{1/n}$  and  $h\nu$  looking for the value of  $n$  (depends on the nature of transition) that gives the best linear fit of a given data set [14]. The allowed direct and indirect transitions are given by the values of  $n$  as  $1/2$  and  $2$ , respectively:

$$\alpha h\nu = A(h\nu - E_{gd})^{1/2},$$

$$\alpha h\nu = B \left[ \frac{(h\nu - E_{gi} + E_p)^2}{\exp(E_p/kT) - 1} + \frac{(h\nu - E_{gi} - E_p)^2}{1 - \exp(-E_p/kT)} \right], \quad (2)$$

where  $A$  and  $B$  are constants,  $E_{gd}$  and  $E_{gi}$  are the direct and indirect energy gaps respectively and  $E_p$  is the phonon energy [13]. All the samples of different concentrations of fullerene polymer composites have the same behavior in their direct and allowed transitions. According to (2), there will be a single straight line for direct transitions and two linear

portions for indirect transitions. It could be observed that from Figure 4(a) plotting  $(\alpha h\nu)^2$  against  $h\nu$  brought in to view a linear behavior that can be considered as an evidence of the direct transition and the optical gap,  $E_{gd}$ , can be estimated from the intercept on the energy axis of the linear fit of the large energy data of the plot [15].

On the other hand, Figure 4(b) shows that plotting  $(\alpha h\nu)^{1/2}$  against  $h\nu$  for indirect transition may be resolved into two distinct straight-line portions. The straight line obtained at lower photon energies, corresponding to phonon-absorption process, cuts the energy axis at  $E_{gi} - E_p$ . The other line represents the dependence in the high energy range corresponding to a phonon-emission process and cuts the energy axis at  $E_{gi} + E_p$ . From the energy intercept of the two straight line portions, the values of  $E_{gi}$  and  $E_p$  could be estimated [14].

The values of  $E_{gd}$ ,  $E_{gi}$ , and  $E_p$  are listed in Table 1 which illustrate that the values of  $E_{gd}$  and  $E_{gi}$  decrease with increasing the concentration of fullerene doped in the polymer sample.

In the mean time, the absorption tails in amorphous and semi crystalline materials could be interpreted in terms of the Dow-Redfield effect [16] taking the form of Urbach rule [17] as follows:

$$\alpha(h\nu) = \alpha_o \exp\left(\frac{h\nu}{E_e}\right), \quad (3)$$

where  $\alpha_o$  is a constant and  $E_e$  is the width of the tail of the localized states in the band gap. The values of  $E_e$  which are listed in Table 1 can be calculated as the reciprocal gradient of the linear portion of plotting  $\ln(\alpha)$  against  $h\nu$ . In addition, Table 1 illustrates that with increasing the concentration of the doped fullerene, the values of  $E_e$  increased. It is noted that

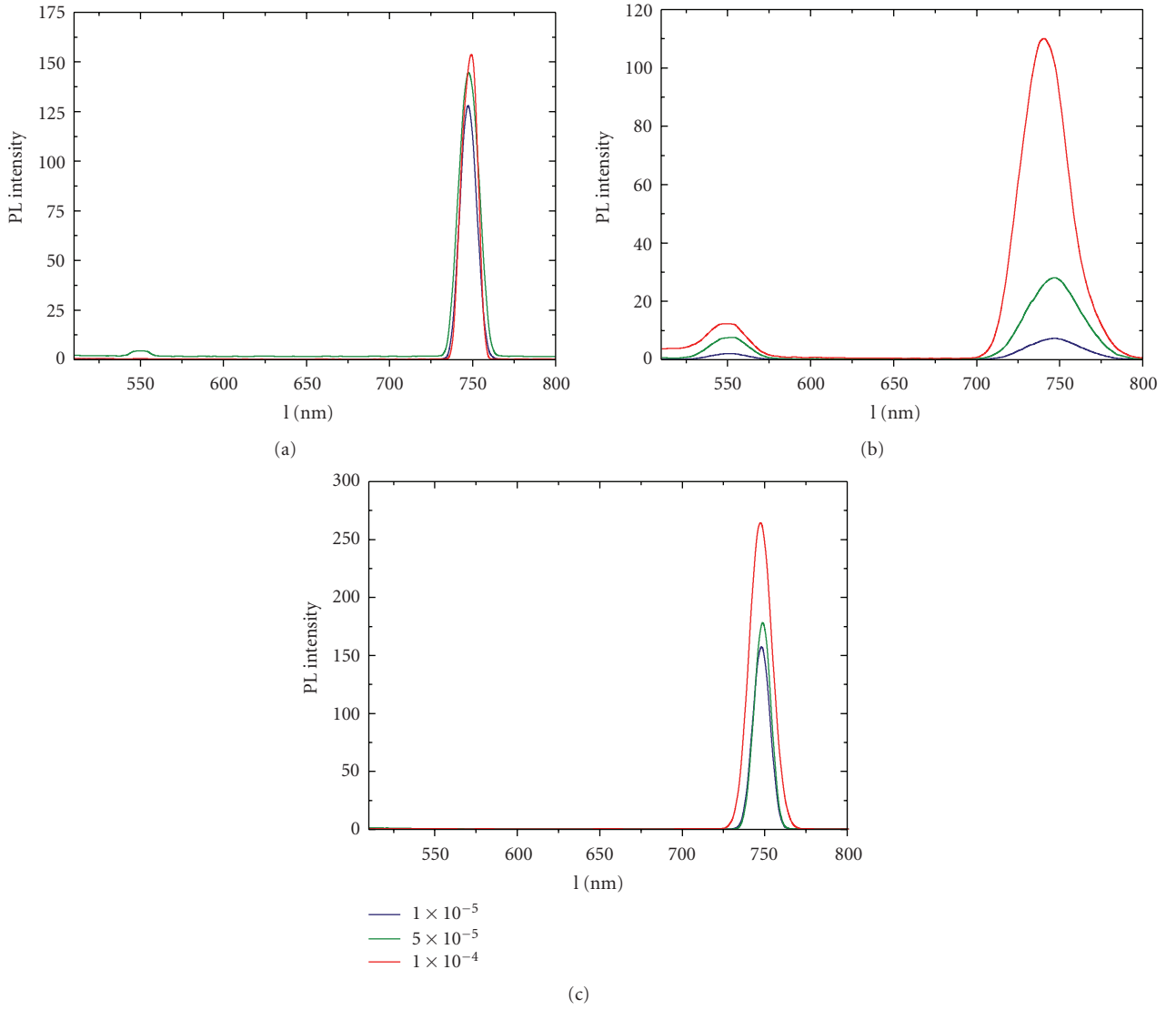


FIGURE 5: Photoluminescence spectra of different concentrations of fullerene doped (a) PMMA, (b) PVAc, and (c) (PMMA/PVAc 50/50) blend excited at 400 nm at the room temperature.

TABLE 1: The values of band tails, optical energy gaps, phonon energy, and the phonon equivalent temperature (given by  $T_p = E_p/k_B$ , where  $k_B$  is Boltzmann's constant, at the room temperature [14]) for different fullerene polymer composites.

| Sample                   | Concentration (mol. %) | $E_{gd}$ (eV) | $E_{gi}$ (eV) | $E_p$ (eV) | $T_p$ (K) | $E_u$ (eV) |
|--------------------------|------------------------|---------------|---------------|------------|-----------|------------|
| $C_{60}$ /PMMA           | $1 \times 10^{-5}$     | 4.80          | 4.00          | 0.32       | 3687      | 0.18       |
|                          | $5 \times 10^{-5}$     | 4.55          | 3.95          | 0.31       | 3572      | 0.19       |
|                          | $1 \times 10^{-4}$     | 4.49          | 3.84          | 0.29       | 3342      | 0.20       |
| $C_{60}$ /PMMA/PVAc50/50 | $1 \times 10^{-5}$     | 5.07          | 4.20          | 0.46       | 4724      | 0.23       |
|                          | $5 \times 10^{-5}$     | 4.85          | 3.17          | 0.38       | 4379      | 0.25       |
|                          | $1 \times 10^{-4}$     | 4.79          | 2.90          | 0.34       | 3918      | 0.25       |
| $C_{60}$ /PVAc           | $1 \times 10^{-5}$     | 5.31          | 3.62          | 0.45       | 5185      | 0.27       |
|                          | $5 \times 10^{-5}$     | 5.26          | 3.28          | 0.45       | 5185      | 0.28       |
|                          | $1 \times 10^{-4}$     | 5.21          | 2.94          | 0.45       | 5185      | 0.29       |

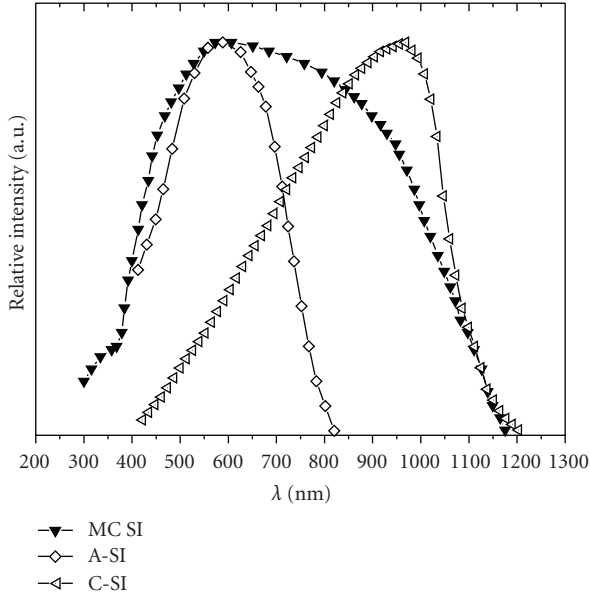


FIGURE 6: The sensitivity of different types of silicon solar cells.

the dependence of  $E_g$  on the sample preparation does not match with  $E_e$  values because the sample having a narrower band gap expected to have a wider band tail. The change in  $E_e$  is probably affected by potential fluctuations associated with the polymer structure but not the change in  $E_g$ , because the initial and final states are practically have the same potential [18].

**3.4. Photoluminescence Spectroscopy of Doped Composites.** The photoluminescence (PL) spectra of different concentrations of fullerene doped in PMMA, PVAc, and their blend, at room temperature, is shown in Figure 5. The full symmetry of  $C_{60}$  molecules is that of the icosahedra point group  $I_h$ , and the highest occupied molecular orbital (HOMO) and the lowest unoccupied molecular orbital (LUMO), of  $C_{60}$  molecules are fivefold-degenerate  $h_u$ , and threefold-degenerate  $t_{1u}$  orbital, respectively. Consequently, the optical transitions between the  $h_u$ -derived valence band and the  $t_{1u}$ -derived conduction band are parity forbidden. However, these transitions can be rendered by either solid state effects or interactions between  $C_{60}$  and surrounding solvent molecules. Thus the PL spectrum for  $C_{60}$ /PMMA films [19] and also that of the others can be interpreted as a result of radiative transitions between the  $h_u$ -derived valence band and the  $t_{1u}$ -derived conduction band. In addition, it is observed that the photoluminescence intensity of the all samples is improved by increasing the concentration of the fullerene doped in the polymer.

Moreover, Figure 5 illustrates that the PL peak intensity for each concentration of  $C_{60}$  doped in (PMMA/PVAc 50/50) blend is greater than the corresponding concentration doped in PMMA and also PVAc composites. Consequently, it could be deduced that (PMMA/PVAc 50/50) blend has modified the optical properties of its homopolymers in agreement with the literature [20]. Also, it is illustrated that there is a

region of PL band centered at  $745 \pm 5$  nm for all the samples. This high luminescence peak of  $C_{60}$  always lies below the transition forbidden HOMO-LUMO gap which depends upon the excitation energy [21]. In addition, a band centered at 550 nm, is observed for fullerene/PVAc composites, which is interpreted as a result of relaxed forbidden transitions of excited carriers between HOMO and LUMO of  $C_{60}$  [19]. The symmetry of  $C_{60}$  is lowered greatly which induces the relaxation of selection rules and a peak of PL [22].

Furthermore, the fluorescence quantum yield has been calculated relative to Rhodamine B as a reference ( $\phi_f = 31\%$  in water) from [23]

$$\Phi_s = \Phi_r \left( \frac{D_s}{D_r} \right) \left( \frac{n_s}{n_r} \right)^2 \left( \frac{1 - 10^{-OD_r}}{1 - 10^{-OD_s}} \right), \quad (4)$$

where  $D_s$  and  $D_r$  are the integrated area under the corrected fluorescence spectra for the sample and reference,  $n_s$  and  $n_r$  are the refractive indices of the sample and reference, respectively. The calculated values for  $\phi_{ref}$  from the lowest to the highest concentration of fullerene are (8, 10, and 13%) for fullerene/PMMA composites, (0.8, 2 and 5%) for fullerene/PVAc composites and (15, 19, and 23%) for fullerene doped in (PMMA/PVAc 50/50) blend. It is clear that the fluorescence quantum yield values strongly depend on the concentration of fullerene doped in the polymer.

Besides this, it is important that the spectral region of sensitivity of the samples luminescence fits the spectral region of sensitivity of the photovoltaic cells. The sensitivity of photovoltaic cell must be adjusted to match the spectral emission of the sample. The spectral sensitivity of silicon is influenced by its production method [24]. Figure 6 shows the spectral sensitivity of some types of silicon solar cells and their range of sensitivity as multicrystalline (MC-SI) from 375 to 1100 nm, amorphous (A-SI) from 410 to 775 nm and crystalline (C-SI) from 500 to 1125 nm. The maximum PL for all the samples as indicated before could be detected by one of these silicon cells.

## 4. Conclusions

Different concentrations of fullerene  $C_{60}$  doped in PVAc, PMMA, and their blend were prepared by solvent casting method. TEM and XRD measurements illustrated that the fullerene doped in the polymer is crystallite. In addition, the phonon energy and the direct and indirect energy gap were calculated for the samples which were decreasing by increasing the concentration of fullerene. On the other hand, the values of the band tail width were inversely proportional to the fullerene concentration as the sample having a narrower band gap expected to have a wider band tail. Moreover, the photoluminescence spectra were detected for the samples which clarified its improvement by increasing the concentration of the fullerene-doped in the polymer as well as the fluorescence quantum yield. Also, PMMA/PVAc blend has modified the optical properties of its homopolymers which is suggested to be a good host matrix for the solar concentrators. Besides, the measured spectral sensitivity of silicon solar cells illustrated the applicability fullerene doped

polymers coatings as luminescent downshifters, to overcome their poor performance at short wavelengths [25].

## Acknowledgments

The authors are grateful the Woman Student Medical Studies and Science Section Research Center of Deanship of Academic Research in King Saud University for Supporting this work.

## References

- [1] A. Tanwar, K. K. Gupta, P. J. Singh, and Y. K. Vijay, "Dielectric parameters and a.c. conductivity of pure and doped poly (methyl methacrylate) films at microwave frequencies," *Bulletin of Materials Science*, vol. 29, no. 4, pp. 397–401, 2006.
- [2] A. Patsidis and G. C. Psarras, "Dielectric behaviour and functionality of polymer matrix—ceramic BaTiO<sub>3</sub> composites," *Express Polymer Letters*, vol. 2, no. 10, pp. 718–726, 2008.
- [3] H. W. Kroto, J. R. Heath, S. C. O'Brien, R. F. Curl, and R. E. Smalley, "C<sub>60</sub>: buckminsterfullerene," *Nature*, vol. 318, no. 6042, pp. 162–163, 1985.
- [4] K. B. Zhogova, I. A. Davydov, V. T. Punin, B. B. Troitskii, and G. A. Domvachiev, "Investigation of fullerene C<sub>60</sub> effect on properties of polymethylmethacrylate exposed to ionizing radiation," *European Polymer Journal*, vol. 41, no. 6, pp. 1260–1264, 2005.
- [5] K. El-Salmawi, M. M. Abu Zeid, A. M. El-Naggar, and M. Mamdouh, "Structure-property behavior of gamma-irradiated poly(styrene) and poly(methyl methacrylate) miscible blends," *Journal of Applied Polymer Science*, vol. 72, no. 4, pp. 509–520, 1999.
- [6] H. M. Zidan, A. Tawansi, and M. Abu-Elnader, "Miscibility, optical and dielectric properties of UV-irradiated poly(vinylacetate)/poly(methylmethacrylate) blends," *Physica B*, vol. 339, no. 2-3, pp. 78–86, 2003.
- [7] G. Ma, W. Cheng, G. Chen, and N. Ming, "Orientation and photoluminescence of C<sub>60</sub> crystallites in C<sub>60</sub>-polymethyl methacrylate films," *Thin Solid Films*, vol. 375, no. 1-2, pp. 292–295, 2000.
- [8] W. C. Oh, A. R. Jung, and W. B. Ko, "Preparation of fullerene/TiO<sub>2</sub> composite and its photocatalytic effect," *Journal of Industrial and Engineering Chemistry*, vol. 13, no. 7, pp. 1208–1214, 2007.
- [9] S. K. J. Al-Ani, Y. Al-Ramadin, M. S. Ahmad et al., "Optical properties of polymethylmethacrylate polymer dispersed liquid crystals," *Polymer Testing*, vol. 18, no. 8, pp. 611–619, 1999.
- [10] A. Miller, *Handbook of Optics*, vol. 1, chapter 9, McGraw-Hill, New York, NY, USA, 1994.
- [11] F. H. Abd El-Kader, W. H. Osman, H. S. Ragab, A. M. Shehap, M. S. Rizk, and M. A. F. Basha, "Electrical and optical properties of polyvinyl alcohol thin films doped with metal salts," *Journal of Polymer Materials*, vol. 21, no. 1, pp. 49–60, 2004.
- [12] F. H. Abd-El Kader, G. Said, G. Attia, and A. M. Abo-El Fadl, "Study of structural and optical properties of ethylene vinyl acetate copolymer films irradiated with  $\gamma$ -Rays," *Search Results Egyptian Journal of Physics*, vol. 37, no. 2, pp. 111–126, 2006.
- [13] J. I. Pankove, *Optical Processes in Semiconductors*, Prentice Hall, Upper Saddle River, NJ, USA, 1972.
- [14] M. A. Gaffar, A. Abu El-Fadl, and S. Bin Anooz, "Electron irradiation-induced effects on optical spectra of (NH<sub>4</sub>)<sub>2</sub>ZnCl<sub>4</sub>: X Sr<sup>2+</sup> single crystals," *Crystal Research and Technology*, vol. 38, no. 1, pp. 83–93, 2003.
- [15] E. Márquez, T. Wagner, J. M. González-Leal et al., "Controlling the optical constants of thermally-evaporated Ge<sub>10</sub>Sb<sub>30</sub>S<sub>60</sub> chalcogenide glass films by photodoping with silver," *Journal of Non-Crystalline Solids*, vol. 274, no. 1, pp. 62–68, 2000.
- [16] J. D. Dow and D. Redfield, "Electroabsorption in semiconductors: the excitonic absorption edge," *Physical Review B*, vol. 1, no. 8, pp. 3358–3371, 1970.
- [17] F. Urbach, "The long-wavelength edge of photographic sensitivity and of the electronic Absorption of Solids," *Physical Review*, vol. 92, no. 5, p. 1324, 1953.
- [18] S. M. El-Bashir, *Preparation and characterization of fluorescent solar concentrators*, M.S. thesis, Zagazig University, Benha, Egypt, 2001.
- [19] G. Ma, Y. Yang, and G. Chen, "Anomalous photoluminescence from C<sub>60</sub>/polymethyl methacrylate films," *Materials Letters*, vol. 34, no. 3–6, pp. 377–382, 1998.
- [20] R. M. Ahmed, "Optical study on poly(methyl methacrylate)/poly(vinyl acetate) blends," *International Journal of Photoenergy*, vol. 2009, Article ID 150389, 7 pages, 2009.
- [21] L. Zhu, Y. Li, J. Wang, and J. Shen, "Structural and optical characteristics of fullerenes incorporated inside porous silica aerogel," *Chemical Physics Letters*, vol. 239, no. 4–6, pp. 393–398, 1995.
- [22] Y. Zhao, Y. Fang, and Y. Jiang, "Fluorescence study of fullerene in organic solvents at room temperature," *Spectrochimica Acta—Part A*, vol. 64, no. 3, pp. 564–567, 2006.
- [23] J. N. Demas and G. A. Crosby, "The measurement of photoluminescence quantum yields. A review," *The Journal of Physical Chemistry*, vol. 75, no. 8, pp. 991–1024, 1971.
- [24] N. Neuroth and R. Haspel, "Glasses for luminescent solar concentrators," *Solar Energy Materials*, vol. 16, no. 1–3, pp. 235–242, 1987.
- [25] E. Klampaftis, D. Ross, K. R. McIntosh, and B. S. Richards, "Enhancing the performance of solar cells via luminescent down-shifting of the incident spectrum: a review," *Solar Energy Materials and Solar Cells*, vol. 93, no. 8, pp. 1182–1194, 2009.



# Hindawi

Submit your manuscripts at  
<http://www.hindawi.com>

